

Evidence of pre-processing and a dependence on dynamical state for low-mass satellite galaxies

Ian D. Roberts,^{*} Laura C. Parker

Department of Physics and Astronomy, McMaster University, Hamilton ON L8S 4M1, Canada

Accepted XXX. Received YYY; in original form ZZZ

ABSTRACT

We study the dependence of satellite star formation rate and morphology on group dynamics for a sample of SDSS groups. We classify the group dynamical state and study satellite properties for populations of galaxies at small and large group-centric radii. For galaxies at large radii we find no differences in the star-forming or disc fraction for those in Gaussian groups compared to those in non-Gaussian groups. By comparing the star-forming and disc fractions of infalling galaxies to field galaxies we find evidence for the pre-processing of both star formation rate and morphology. The strength of pre-processing increases with halo mass and is highest for low-mass galaxies infalling onto high-mass haloes. We show that the star formation rate of galaxies at small radii correlates with group dynamical state, with galaxies in non-Gaussian groups showing enhanced star-forming fractions compared to galaxies in Gaussian groups. Similar correlations are not seen for the disc fractions of galaxies at small radii. This seems to suggest that either the mechanisms driving star formation quenching at small halo-centric radii are more efficient in dynamically relaxed groups, or that non-Gaussian groups have assembled more recently and therefore satellites of the groups will have been exposed to these transforming mechanisms for less time.

Key words: galaxies: clusters: general – galaxies: evolution – galaxies: groups: – galaxies: statistics

1 INTRODUCTION

In the first half of the twentieth century it was beginning to be realized that populations of high-mass clusters were predominantly made up of early-type galaxies, with Hubble & Humason (1931) stating that, “The predominance of early types is a conspicuous feature of clusters in general”. Many subsequent observational studies have cemented the now familiar environmental dependence of galaxy properties (e.g. Butcher & Oemler 1978; Dressler 1980; Postman & Geller 1984; Dressler et al. 1999; Blanton et al. 2005; Wetzel et al. 2012). Namely, galaxies in clusters tend to be red in colour with low star formation rates and early-type morphologies. On the other hand the low-density field is preferentially populated by blue, star forming, spiral galaxies. A third environment, galaxy groups, are the most common environment in the local Universe (Geller & Huchra 1983; Eke et al. 2005) and also represent an intermediate-mass regime in which significant populations of both star-forming spirals and passive ellipticals are observed (e.g. Wilman et al. 2005; McGee et al. 2011).

Not only do galaxy properties correlate with the type

of haloes in which they reside, but also with distance from the halo centre. In particular, galaxies at large radii show enhanced star formation and are more likely to have spiral morphologies compared to galaxies near the centre of the halo (Whitmore et al. 1993; Goto et al. 2003; Postman et al. 2005; Rasmussen et al. 2012; Wetzel et al. 2012; Fasano et al. 2015; Haines et al. 2015). Therefore, in order to probe the environmentally driven aspects of galaxy evolution it is crucial to account for both the dependence on the host halo environment as well as the radial position within the group or cluster.

The aforementioned environmental dependences are strongest for low-mass galaxies and it appears that properties of high-mass galaxies are less dependent on environment (Haines et al. 2006; Bamford et al. 2009). For high-mass galaxies, quenching is thought to be driven by internal, secular processes such as feedback from AGN (e.g. Schawinski et al. 2009). This dichotomy between high and low mass galaxies is presented in Peng et al. (2010) where it is argued that in the local Universe galaxies below $\sim 10^{10.5} M_{\odot}$ are environmentally quenched as satellite galaxies and galaxies above that mass are primarily quenched by internal processes (so-called “mass quenching”).

While it appears that the majority of low-mass galax-

^{*} E-mail: roberid@mcmaster.ca

ies are primarily quenched as satellites, there are still open questions regarding the details of the process(es) involved. One such question is which are the dominant mechanism(s) responsible for suppressing star formation in satellite galaxies? Galaxy harassment (e.g. Moore et al. 1996), mergers (e.g. Mihos & Hernquist 1994), starvation (e.g. Kawata & Mulchaey 2008), and ram-pressure stripping (e.g. Gunn & Gott 1972) have all been invoked, however no consensus exists on their relative importance in different environments. Additionally, while all of these mechanisms are capable of quenching galaxies (either through inducing rapid star formation and thus quickly using up cold gas reserves, or the stripping of gas), not all would have a strong effect on galaxy morphology. Recently, starvation and/or ram-pressure stripping are often favoured as satellite quenching mechanisms (Muzzin et al. 2014; Peng et al. 2015; Fillingham et al. 2015; Weisz et al. 2015; Wetzel et al. 2015) but it is not clear that either would strongly impact morphology, therefore in order to explain the observed correlation between galaxy star formation and morphology it seems that an additional process to efficiently drive morphological transformations is perhaps required (e.g. Christlein & Zabludoff 2004).

Also of importance is determining the characteristic haloes in which most satellite galaxies are quenched and experience morphological transformations. Do galaxies remain actively forming stars with late-type morphologies until passing the virial radius of high-mass clusters, or are they transformed in smaller groups prior to or during cluster infall (known as “pre-processing”) (e.g. Fujita 2004). Pre-processing is often invoked to explain observational results such as passive and red fractions at large cluster-centric radii which are enhanced significantly relative to the field (Lu et al. 2012; Wetzel et al. 2012; Bahé et al. 2013; Haines et al. 2015; Just et al. 2015), as well as the prevalence of S0 galaxies in large clusters (Kodama & Smail 2001; Helsdon & Ponman 2003; Moran et al. 2007; Wilman et al. 2009). Studies have also found evidence for pre-processing by measuring the fraction of galaxies which are part of a group subhalo during infall onto a cluster, both using simulations (McGee et al. 2009; De Lucia et al. 2012; Bahé et al. 2013) and observations (Dressler et al. 2013; Hou et al. 2014).

This pre-processing and recent infall of galaxies can imprint itself on the dynamical profile of a group or cluster. For a dynamically relaxed group it is expected that the projected velocity profile of member galaxies will resemble a Gaussian distribution whereas groups which are dynamically young and unrelaxed tend to display velocity profiles which are less Gaussian in nature (e.g. Yahil & Vidal 1977; Bird & Beers 1993; Martínez & Zandivarez 2012; Ribeiro et al. 2013a). The degree to which galaxy properties correlate with the dynamical state of their host groups is still an open question (e.g. Biviano et al. 2002; Ribeiro et al. 2013b), though it may be expected that such correlations exist. For example, dynamically complex groups are preferentially X-ray underluminous (Popesso et al. 2007; Roberts et al. 2016) which indicates an underdense intra-group medium. Considering that many quenching mechanisms operate through interactions with the intra-group medium it may be expected that such mechanisms will be less efficient in non-Gaussian groups. Furthermore, if non-Gaussian groups represent younger systems then galaxy properties could be affected (compared to Gaussian systems) simply due to galaxies being exposed to

a dense environment for less time. Previous work has suggested that galaxies in relaxed groups tend to be redder than galaxies in unrelaxed groups (Ribeiro et al. 2010; Carollo et al. 2013; Ribeiro et al. 2013a). However less work has been done studying the dynamical dependences of star formation and morphology directly. One example is the work of Hou et al. (2013) who find no detectable difference between the quiescent fractions of galaxies in Gaussian versus non-Gaussian groups as a function of redshift.

Previously we have shown that the star formation and morphology of low-mass galaxies depends not only on stellar and halo mass but also on the X-ray luminosity of the host group (Roberts et al. 2016). Here we investigate the dependence of star-forming and morphological properties of galaxies on group dynamical state. In particular, we study these properties within different radial regions of the halo to explore whether galaxy properties correlate with group dynamical state and whether any correlations show radial dependence.

The outline of this paper is as follows. In Section 2 we describe the sample of galaxies in groups as well as our field sample. In Section 3 we analyze the dependence of galaxy star formation and morphology on dynamics for galaxies at large radii. In Section 4 we do the same for galaxies in the inner regions of the halo. We discuss our results in Section 5 and summarize in Section 6.

In this paper we assume a flat Λ cold dark matter cosmology with $\Omega_M = 0.3$, $\Omega_\Lambda = 0.7$, and $H_0 = 70 \text{ km s}^{-1} \text{ Mpc}^{-1}$.

2 DATA

2.1 Group sample

For this work we employ the group catalogue of Yang et al. (2007), which is constructed by applying the halo-based galaxy group finder from Yang et al. (2005, 2007) to the New York University Value-Added Galaxy Catalogue (NYU-VAGC; Blanton et al. 2005). The NYU-VAGC is a low redshift galaxy catalogue consisting of ~ 700000 galaxies in the Sloan Digital Sky Survey Data Release 7 (SDSS-DR7; Abazajian et al. 2009). We will briefly describe the halo-based group finding algorithm used to generate the Yang group catalogue, however for a more complete description please see Yang et al. (2005) and Yang et al. (2007).

First, the centres of potential groups are identified. Galaxies are initially assigned to groups using a traditional “friends-of-friends” (FOF) algorithm (e.g. Huchra & Geller 1982) with very small linking lengths. The luminosity-weighted centres of FOF groups with at least two members are then taken as the centres of potential groups and all galaxies not yet associated with a FOF group are treated as tentative centres for potential groups. A characteristic luminosity, $L_{19.5}$, defined as the combined luminosity of all group members with $^{0.1}M_r - 5 \log h \leq -19.5$, is calculated for each tentative group and an initial halo mass is assigned using an assumption for the group mass-to-light ratio, $M_H/L_{19.5}$. Utilizing this tentative group halo mass, velocity dispersions and a virial radius are calculated for each group. Next, galaxies are assigned to groups under the assumption that the distribution of galaxies in phase space follows that of dark matter particles – the distribution of dark matter particles

is assumed to follow a spherical NFW profile (Navarro et al. 1997). Using the new group memberships, group centres are recalculated and the procedure is iterated until group memberships no longer change.

We take group halo masses, M_H , from the Yang catalogue calculated using a characteristic group stellar mass, $M_{*,\text{grp}}$, and assuming that there is a one-to-one relation between $M_{*,\text{grp}}$ and M_H . Yang et al. (2007) define $M_{*,\text{grp}}$ as

$$M_{*,\text{grp}} = \frac{1}{g(L_{19.5}, L_{\text{lim}})} \sum_i \frac{M_{*,i}}{\mathcal{C}_i} \quad (1)$$

where $M_{*,i}$ is the stellar mass of the i th member galaxy, \mathcal{C}_i is the completeness of the survey at the position of that galaxy, and $g(L_{19.5}, L_{\text{lim}})$ is a correction factor which accounts for galaxies missed due to the magnitude limit of the survey. While we utilize halo masses derived from group stellar mass in this paper, we have run the same analysis using halo masses derived from group luminosity in the Yang catalogue and see no changes in observed trends. Campbell et al. (2015) show that the choice between stellar mass and luminosity as a halo mass predictor can introduce biases in mass estimates. For example, when group luminosity is assumed to be the primary property determining halo occupation in mock catalogues, halo masses inferred from group stellar mass are systematically larger for haloes with a red central compared to haloes with a blue central (Campbell et al. 2015). For the samples of Gaussian and non-Gaussian groups which are frequently compared in this paper (see Section 2.3), we find that the fraction of groups with passive centrals is 94 per cent in both cases, therefore the aforementioned effects should not preferentially bias one sample more than the other.

The Yang catalogue contains both haloes which would be broadly classified as groups ($10^{12} \lesssim M_H \lesssim 10^{14} M_\odot$) as well as clusters ($M_H \gtrsim 10^{14} M_\odot$), however for brevity we will refer to all haloes as groups regardless of halo mass unless otherwise specified.

We calculate group-centric radii for all group members within the sample using the redshift of the group and the angular separation of the galaxy from the luminosity-weighted centre of the host halo. Radii are normalized by the virial radius, R_{200} , of the group which is defined as (Yang et al. 2007; Tinker et al. 2008):

$$R_{200} = \left[\frac{M_H}{200(4/3)\pi\Omega_{m,0}\rho_{c,0}(1+z)^3} \right]^{1/3}. \quad (2)$$

For the cosmology assumed in this work, equation 2 becomes

$$R_{200} = 1.13 h^{-1} \text{Mpc} \left(\frac{M_H}{10^{14} h^{-1} M_\odot} \right)^{1/3} (1+z_{\text{group}})^{-1}. \quad (3)$$

For our group sample, we consider galaxies which have projected group-centric radii within R_{200} .

To study specific characteristics of galaxies within the group sample, we match various public SDSS galaxy catalogues to the group sample. We utilize galaxy stellar masses and k-corrected absolute magnitudes given in the NYU-VAGC, which are obtained through fits to galaxy spectra and broadband photometric measurements following the procedure of Blanton & Roweis (2007).

For our star formation indicator we use fibre-corrected specific star formation rates ($SSFR = SFR/M_*$) from the MPA-JHU DR7 catalogue (Brinchmann et al. 2004). These SSFRs are primarily derived from emission lines, with an exception for galaxies with no clear emission lines or AGN contamination in which case SSFRs are based on the 4000 Å break. SSFRs for galaxies with $S/N > 2$ in $H\alpha$ are determined using only the $H\alpha$ line and SSFRs for galaxies with $S/N > 3$ in all four BPT lines are determined using a combination of emission lines. For this work we define star-forming galaxies to be all galaxies with $\log SSFR \geq -11$, Wetzel et al. (2012) show that in the local Universe the division between the red sequence and the blue cloud is consistently found at $\log SSFR \simeq -11$ across a wide range of halo masses.

For our morphology indicator we use a global Sérsic index, n , taken from the single component Sérsic fits in Simard et al. (2011), and define disc galaxies as all galaxies with $n \leq 1.5$. While the distribution of Sérsic index is not as clearly bimodal as the SSFR distribution, we find that our observed trends are insensitive to our exact choice of dividing Sérsic index. We also weight all of the data by $1/V_{\text{max}}$ as given in Simard et al. (2011) to account for the stellar-mass incompleteness of the sample. This does not explicitly account for the fact that completeness is also a function of galaxy colour, with star-forming galaxies being visible at higher redshift than passive galaxies (e.g. Taylor et al. 2011). While the sample will be biased towards detecting star-forming galaxies at high redshift, we do not expect that this bias will affect galaxies in Gaussian groups differently than galaxies in non-Gaussian groups. Furthermore, the fact that we match all samples by redshift (see Section 2.4) should help to ensure that the completeness (as a function of colour) of the different galaxy samples does not vary substantially. We note that we do not use a stellar mass complete sample in this work due to the fact that the sample size would be significantly reduced, and in particular, the sample of galaxies in non-Gaussian groups would be very small.

For our analysis we consider only satellite galaxies within groups. Central galaxies are defined as the most-massive galaxy (MMG) within a group and subsequently removed from the data set. We note that it has been shown that the most-massive (or brightest) group galaxy does not always correspond to the group central (ie. the galaxy closest to the centre of the potential), for example Skibba et al. (2011) show that the fraction of galaxies which are brightest but do not reside at the centre of the potential ranges from ~ 25 per cent for group-mass haloes to ~ 40 per cent for high-mass clusters. To gauge any potential influence that removing the MMG has on the results, we repeat the analysis both with no removal of the MMG and also with removing the second most-massive galaxy instead of the MMG. In both cases, this does not alter the observed trends qualitatively or quantitatively.

To ensure reasonable statistics when classifying the dynamical states of the groups (see Section 2.3) we only include groups from the Yang catalogue which have eight or more member galaxies. In total, this gives an initial group sample of 47961 galaxies in 2662 groups.

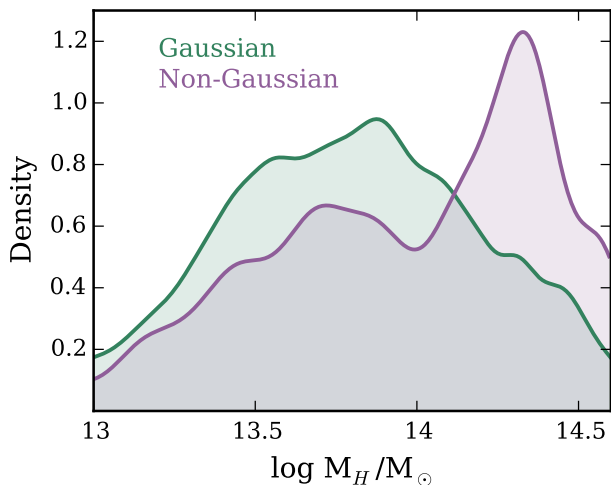


Figure 1. Halo mass distributions, smoothed using a Gaussian kernel, for galaxies in the unmatched G and NG samples.

2.2 Infalling and field samples

We also define samples of “infalling” and “field” galaxies, for further comparisons.

To populate the infalling sample we take all galaxies in single-member groups from the Yang catalogue which have projected distances from luminosity-weighted group centres between 1 and 3 virial radii, and have line-of-sight (LOS) velocities less than 1.5σ from the group centroid, where velocity dispersions, σ , are calculated using Equation 6 from Yang et al. (2007). We further define a ‘strict’ infalling sample with the same velocity threshold but only containing galaxies between 2 and 3 virial radii. Galaxies which satisfy this criteria for multiple groups, are assigned as infalling onto the group which they are closest to. This results in a sample of 19598 galaxies infalling onto 2396 groups.

Our field sample is defined as all galaxies in single-member groups which are not members of the infalling sample, and are separated from their nearest ‘bright’ neighbour by at least 1 Mpc in projected distance and 1000 km s^{-1} in LOS velocity, though our results are insensitive to the exact isolation criteria chosen. We define bright neighbours as all galaxies which are brighter than the survey r-band absolute magnitude limit at $z = 0.2$ (our redshift upper limit), which corresponds to $M_{r,\text{lim}} = -21.3$. Without this condition, the strictness of our isolation criteria would vary with redshift. We also remove any galaxies which are within 1 Mpc of a survey edge, or are within 1000 km s^{-1} of our maximum redshift to ensure that all galaxies truly satisfy the isolation criteria. This yields a field sample consisting of 352262 galaxies.

Stellar masses, absolute magnitudes, SSFRs, and Sérsic indices for the infall and field sample are obtained from the same sources discussed in Section 2.1.

2.3 Group dynamics

To classify the dynamical state of the haloes in the data set we use a combination of two statistical tests, the Anderson-Darling (AD) normality test (Anderson & Darling 1952; see

Hou et al. 2009, 2013 for an astronomical application) and the Dip test (Hartigan & Hartigan 1985; see Ribeiro et al. 2013a for an astronomical application).

The AD test is a non-parametric test of normality based upon the comparison between the cumulative distribution function (CDF) of a measured data sample and the CDF of a Gaussian distribution. Under the assumption that the data is in fact normally distributed, the AD test determines the probability (p) that the difference between the CDFs of the data and a normal distribution equals or exceeds the observed difference. We apply the AD test to the velocity distributions of the member galaxies of each group in the sample, thereby broadly classifying the dynamical state of each halo. Our first criteria in classifying a group as Gaussian (G) is that the p-value given by the AD test be greater than or equal to 0.05.

Our second criteria required for a group to be classified as G is that its velocity distribution be unimodal. Ideally standard normality tests would detect all instances of multimodality, however this is not always the case. In particular, multimodality in distributions with modes at small separations can be missed by standard statistical techniques (Ashman et al. 1994). To gauge the modality of the velocity distribution of a given group we use the Dip test. Like the AD test, the Dip test is also a non-parametric CDF statistic. Where they differ is that the Dip test looks for a flattening of the CDF for the data which would correspond to a ‘dip’ in the distribution being tested. The Dip test operates under the null hypothesis that the data is unimodal, and we consider a group velocity distribution unimodal if the Dip test p-value is greater than or equal to 0.05. Therefore our G data sample consists of all those groups with $p_{\text{ad}} \geq 0.05$ and $p_{\text{dip}} \geq 0.05$, whereas our non-Gaussian (NG) data sample consists of all those groups with $p_{\text{ad}} < 0.05$ or $p_{\text{dip}} < 0.05$.

After applying the above criteria we find a G sample consisting of 42655 galaxies within 2447 groups and a NG sample consisting of 5306 galaxies within 215 groups. We find that the AD test is the stronger discriminator compared to the Dip test as out of all of the galaxies making up the NG sample, 90 per cent failed the AD test but passed the Dip test, 8 per cent passed the AD test but failed the Dip test, and 2 per cent failed both the AD test and the Dip test. The authors note that it is easier to statistically identify NG groups for groups with high galaxy membership, this can lead to the NG sample being skewed toward large halo masses (see Fig. 1). To address this we match our G and NG samples by halo mass (as well as stellar mass and redshift), as described in the following section.

2.4 Matched data set

To ensure a fair comparison between galaxies in different environments (ie. field galaxies, infall galaxies, galaxies in G groups, and galaxies in NG groups) we match our sample of G group galaxies, NG group galaxies, and infalling galaxies by stellar mass, redshift, and halo mass¹. Additionally, we then match our sample of field galaxies by stellar mass and

¹ Though galaxies in the infall sample are not identified as group members, we match them by the halo mass of the group they are nearest to in projection

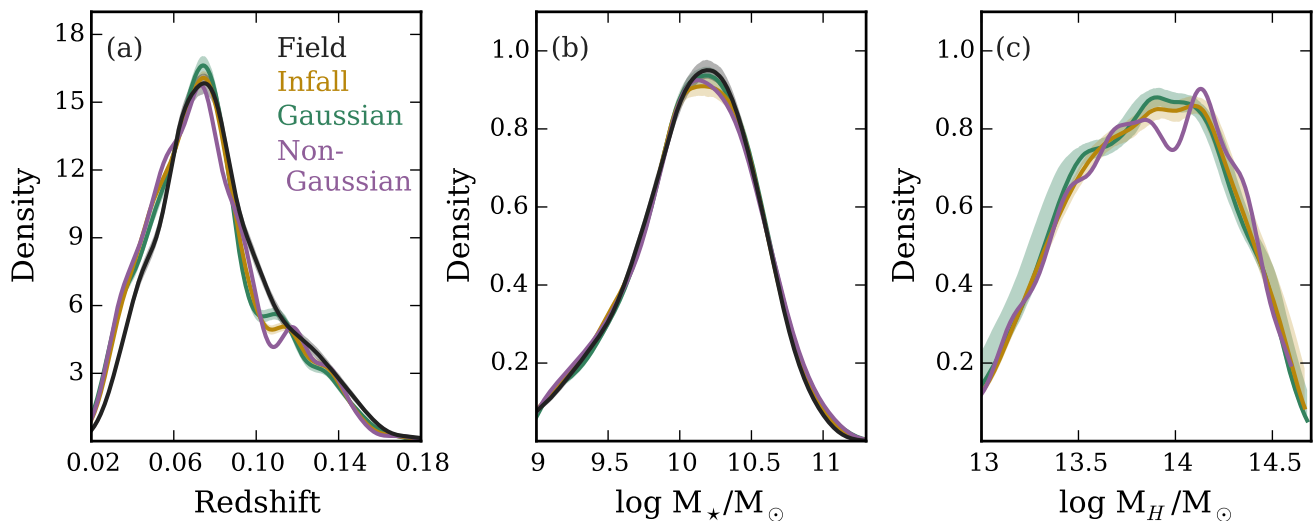


Figure 2. Distributions for stellar mass, redshift, and host halo mass for galaxies in the matched G, NG, infall, and field (where applicable) samples, smoothed using a Gaussian kernel. Shaded regions around the G, infall, and field lines are 99 per cent Monte Carlo confidence intervals corresponding to the stochastic nature of our matching procedure. The lines corresponding to the NG sample have no shading because it is the NG sample to which the other samples are stochastically matched.

redshift. The matching is particularly important when trying to elucidate information on the effect of group dynamics on galaxy star formation and morphological properties for two main reasons:

First, stellar mass, redshift, and halo mass have all been shown to influence galaxy star formation and morphology (e.g. Brinchmann et al. 2004; Feulner et al. 2005; Zheng et al. 2007; Cucciati et al. 2012; Wetzel et al. 2012; Lackner & Gunn 2013; Tasca et al. 2014); whereas the impact of group dynamics is less clear (Hou et al. 2013; Ribeiro et al. 2013a) which is suggestive of a more modest role. Therefore, to search for trends in galaxy star formation and morphology with group dynamics it is crucial to properly control for these other known correlations.

Second, standard statistical normality tests, such as the AD test, are biased towards identifying non-Gaussian distributions when sample size is large. This is a result of the statistical power of the test increasing with sample size which subsequently allows the detection of more and more subtle departures from normality (Razali & Wah 2011). While these subtle departures from normality will perhaps be statistically significant, they may not be physically relevant (in principle, no group is perfectly Gaussian) and what really matters is whether galaxies in groups which show large departures from normality have different properties than galaxies in groups which show smaller departures from normality. Since group richness generally scales with halo mass, in the absence of any matching procedure, a sample of NG groups will be biased towards large halo masses compared to a similar sample of G groups – even though many high halo mass NG groups may have been identified on the basis of very small departures from normality. Ensuring that our G and NG samples have similar halo mass distributions allows us to make a fairer comparison between the two samples.

Our algorithm for matching the G and NG samples is as follows:

1. Our list of galaxies found in NG groups is iterated through, for each galaxy one ‘matching’ galaxy from the G sample is found. To be considered matching the two galaxies must have stellar masses within 0.1 dex, redshifts within 0.01, and halo masses within 0.1 dex.

2. Step 1 is repeated until no more matches are found. The end result is a list of galaxies from the NG sample each of which will have one or more matching galaxies from the G sample assigned to them

3. The matched G sample is generated by including two galaxies from the G sample for every one matching galaxy from the NG sample. By definition this excludes any galaxies in the NG sample which only have one identified match. However, 85 per cent of galaxies in the NG sample have two or more matches so although we reduce the NG sample size by 15 per cent it allows us to increase the matched G sample size twofold. It is worth noting that when we run our analysis keeping only one matched G galaxy instead of two, we find no changes in the trends observed.

4. In the case where a given galaxy in the NG sample has more than two identified matches, the two matching galaxies from the G sample are chosen randomly. This introduces a stochastic nature to our analysis as each generation of the matched G sample will not contain exactly the same galaxies. To account for this, any quantities calculated using the matched G sample are done so in a Monte Carlo sense where the median of 1000 stochastic generations is quoted.

The infall and field sample are subsequently matched to the NG sample following the same procedure and the same method is used to account for the stochastic nature of the matching procedure. Fig. 2 shows smoothed density distributions of stellar mass, redshift, and halo mass for the matched G, NG, infall, and field samples. For the remainder of the paper all analysis is done using the matched samples, there-

fore from this point forward any reference to the G, NG, infall, or field samples refers to the matched samples.

3 GALAXY PROPERTIES AT LARGE RADII

We first consider the star-forming and morphological properties of galaxies at large group-centric radii, and for comparison show the same trends for galaxies within the infall and field samples. We separate galaxies at large and small radii at $1/2R_{200}$ which is close to the median group-centric radius for the sample of $0.43R_{200}$. We apply a lower stellar mass cut at $10^{9.5}M_{\odot}$ in order to avoid including galaxies with large $1/V_{\max}$ weights.

In Fig. 3 we show star-forming ($\log\text{SSFR} > -11$) and disc ($n < 1.5$) fractions versus stellar mass for the four different galaxy samples. The bottom panels show the difference in star-forming/disc fractions between the NG and G samples ($\text{NG} - \text{G}$) coarsely binned into low-mass ($M_{\star} < 10^{10.2}M_{\odot}$) and high-mass ($M_{\star} > 10^{10.2}M_{\odot}$) galaxies, where $10^{10.2}M_{\odot}$ is the median stellar mass of the sample. We estimate uncertainties on star-forming and disc fractions using two methods. First, we follow Cameron (2011) who advocate the use of Bayesian binomial confidence intervals derived from the quantiles of the beta distribution to estimate statistical uncertainties on population fractions. The error bars on the fractions correspond to 68 per cent confidence intervals obtained using this method. Second, we quote 68 per cent bootstrap confidence intervals derived by bootstrapping over the member galaxies of individual groups, the confidence intervals derived from 1000 bootstrap realizations are shown as shaded regions.

In Fig. 3 we see a distinct trend in terms of star-forming and disc fractions, where field galaxies show the highest fractions, followed by infalling galaxies, followed by large-radius group members. Focusing now on the two dynamical samples we see no systematic difference between the star-forming or disc fractions for galaxies at large-radii within G groups compared to galaxies in NG groups. This suggests that any influence that the dynamical state of the group has on star-forming or morphological properties is not in place at large radii within the groups. This is apparent in the lower panels of Fig. 3 where the value of $\text{NG} - \text{G}$ is consistent with zero for both star-forming and disc fractions, regardless of stellar mass. As stated in Section 2.3 we have used a p-value of 0.05 to divide the sample into G and NG groups, however we note that the results in Fig. 3 are not sensitive to the specific choice from a reasonable range of p-values (see Appendix A).

We also see that the star-forming and disc fractions for galaxies at large radii are significantly below the values for the field sample. Previous studies (Lewis et al. 2002; Gray et al. 2004; Rines et al. 2005; Verdugo et al. 2008) have similarly found that star formation of galaxies within infall regions remains suppressed compared to the field out to radii of $\sim 2 - 3R_{200}$. This suppression is often attributed to backplash galaxies which have already made a passage through the halo centre, the pre-processing of galaxies in small groups prior to infall, or some combination of the two. We are particularly interested in determining how much of this difference can be accounted for by pre-processing. It is expected that pre-processing should play a more impor-

tant role in large clusters compared to smaller groups, as a larger fraction of galaxies infalling onto clusters will have been a part of a group prior to infall. This is a result of the hierarchical build-up of structure; regions of space around large clusters are not average but are preferentially populated with other dense structures such as group haloes (e.g. Mo & White 1996; Wang et al. 2008).

We look for evidence of pre-processing by examining the ‘‘field excess’’, which we define as the difference in star forming or disc fraction between field and infalling galaxies at a given stellar mass, for different halo mass ranges. The range in group-centric radii for galaxies in the infall sample ($1 < R < 3R_{200}$) is susceptible to contamination from galaxies backslashing beyond the virial radius after first pericentric passage (e.g. Bahé et al. 2013). To address this, we also show pre-processing results for our ‘strict’ infall sample ($2 < R < 3R_{200}$) which should be less susceptible to backslash contamination, as many previous studies have shown that the majority of backslashing galaxies are found within two virial radii (Mamon et al. 2004; Mahajan et al. 2011; Oman et al. 2013; Haines et al. 2015). If contamination from backslash galaxies is low, this field excess should approximate the fraction of galaxies which have been pre-processed prior to infalling onto their present-day group. We investigate the halo mass dependence of pre-processing by splitting the group sample into three halo mass bins each containing an approximately equal number of galaxies: $10^{13} < M_H \leq 10^{13.7}M_{\odot}$, $10^{13.7} < M_H \leq 10^{14.1}M_{\odot}$, and $10^{14.1} < M_H \leq 10^{15}M_{\odot}$, as well as two stellar mass bins (for each range in halo mass): $M_{\star} < 10^{10.2}M_{\odot}$ and $M_{\star} > 10^{10.2}M_{\odot}$. In Fig. 4 we show the percentage of low-mass and high-mass galaxies which have been pre-processed in terms of star-forming fraction and disc fraction, and its dependence on halo mass, for the infall sample (filled markers) and the strict infall sample (open markers).

For low-mass galaxies we detect modest, but statistically significant, pre-processing of both star formation and morphology (Fig. 4a). At low stellar mass, the pre-processing of star formation tends to increase with halo mass, while the pre-processing of morphology shows a weaker halo mass trend. Pre-processing trends for high-mass galaxies (both in terms of the magnitude of pre-processing, and halo mass trends) are much weaker.

4 GALAXY PROPERTIES AT SMALL RADII

We now consider star-forming and disc fractions for galaxies at small radii within the halo, and again consider the differences between the G, NG, infall, and field samples. Fig. 5 shows star-forming and disc fractions versus stellar mass for the four galaxy samples. In contrast to the outer region of the halo, when considering star-forming fractions for galaxies at small radii a dependence on group dynamics emerges. In particular, galaxies in G groups have the lowest star-forming fractions and galaxies in NG groups have intermediate values – larger star-forming fractions than galaxies in G groups but significantly smaller than infalling galaxies or the field. As shown in the lower panels of Fig. 5, this difference between G and NG groups is significant for low mass galaxies (2.9σ) but not for high mass galaxies (1.6σ). When considering disc fraction, we do not detect a signifi-

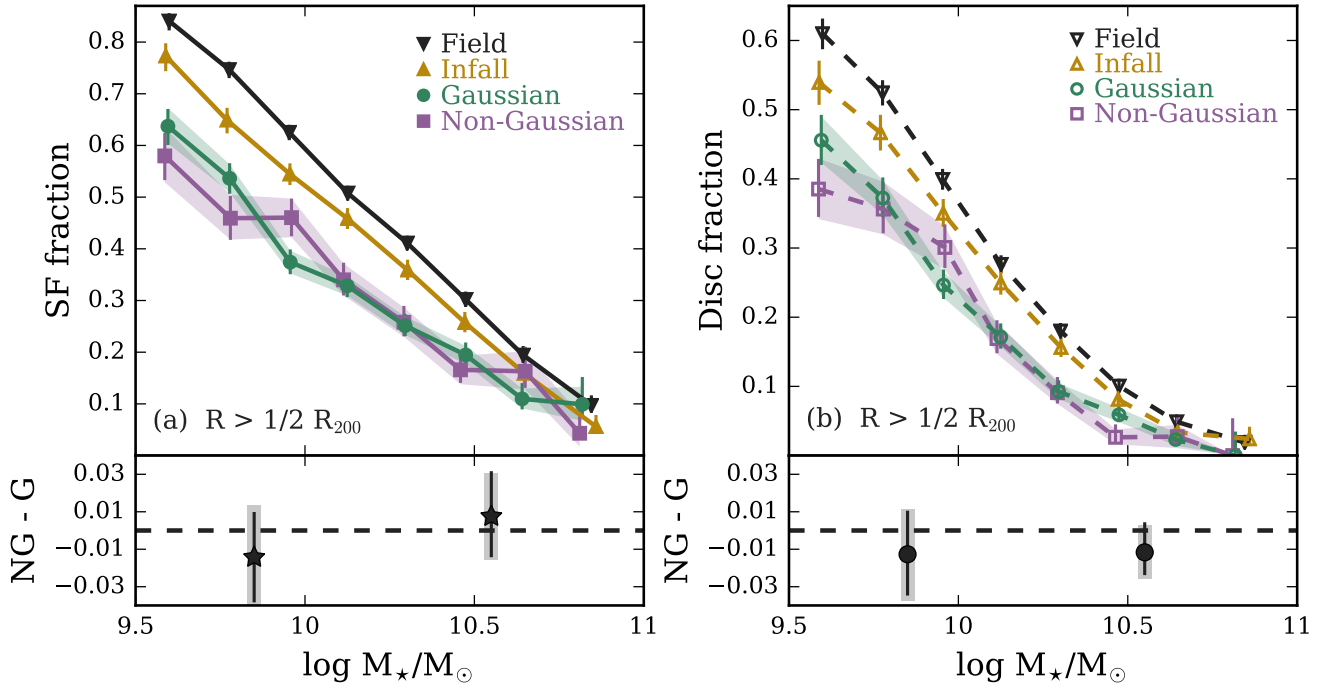


Figure 3. Star-forming (left) and disc (right) fraction versus stellar mass for field galaxies, infalling galaxies, and galaxies at large radii (outside $1/2 R_{200}$) in the G and NG samples. Error bars correspond to 68 per cent binomial confidence intervals as given in Cameron (2011), shaded regions are 68 per cent confidence intervals derived from 1000 bootstrap re-samplings over individual groups. Lower panels show the difference in star-forming/disc fractions between G and NG groups, for low-mass ($M_* \lesssim 10^{10.2} M_\odot$) and high-mass ($M_* \gtrsim 10^{10.2} M_\odot$) galaxies.

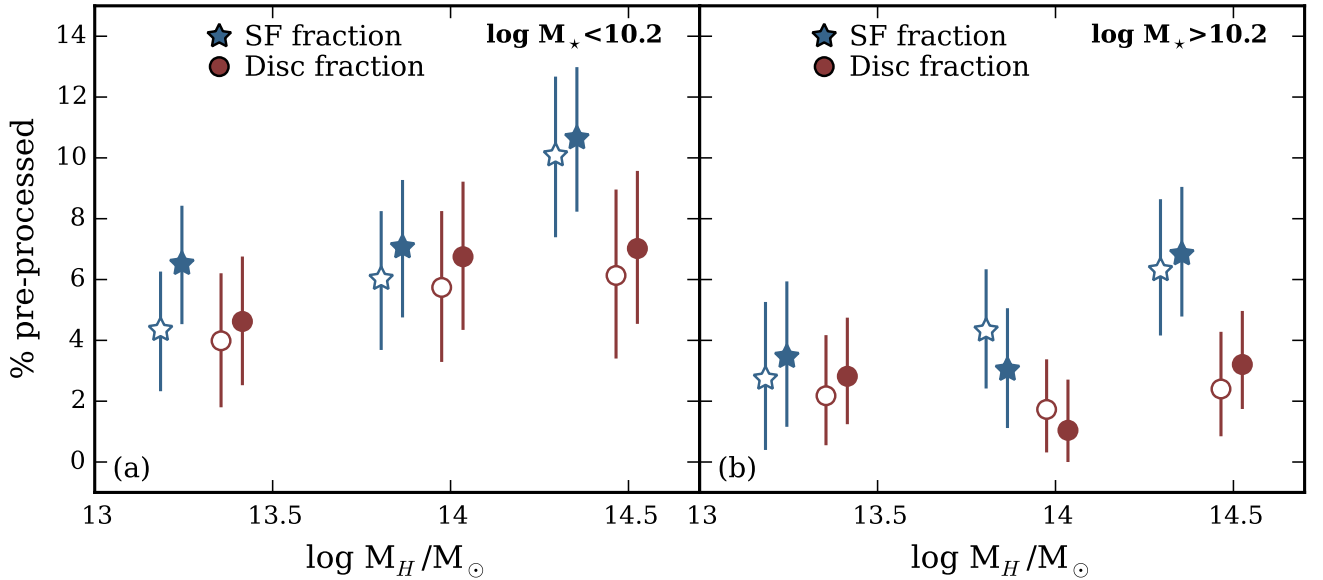


Figure 4. Percentage of infalling galaxies which have had star formation (stars) or morphology (circles) pre-processed for both low-mass ($M_* < 10^{10.2} M_\odot$, left) and high-mass ($M_* > 10^{10.2} M_\odot$, right) galaxies, as a function of halo mass. Filled markers correspond to the whole infall sample ($1 < R < 3 R_{200}$) and open markers correspond to the strict infall sample ($2 < R < 3 R_{200}$). Error bars are 68 per cent binomial confidence intervals (Cameron 2011).

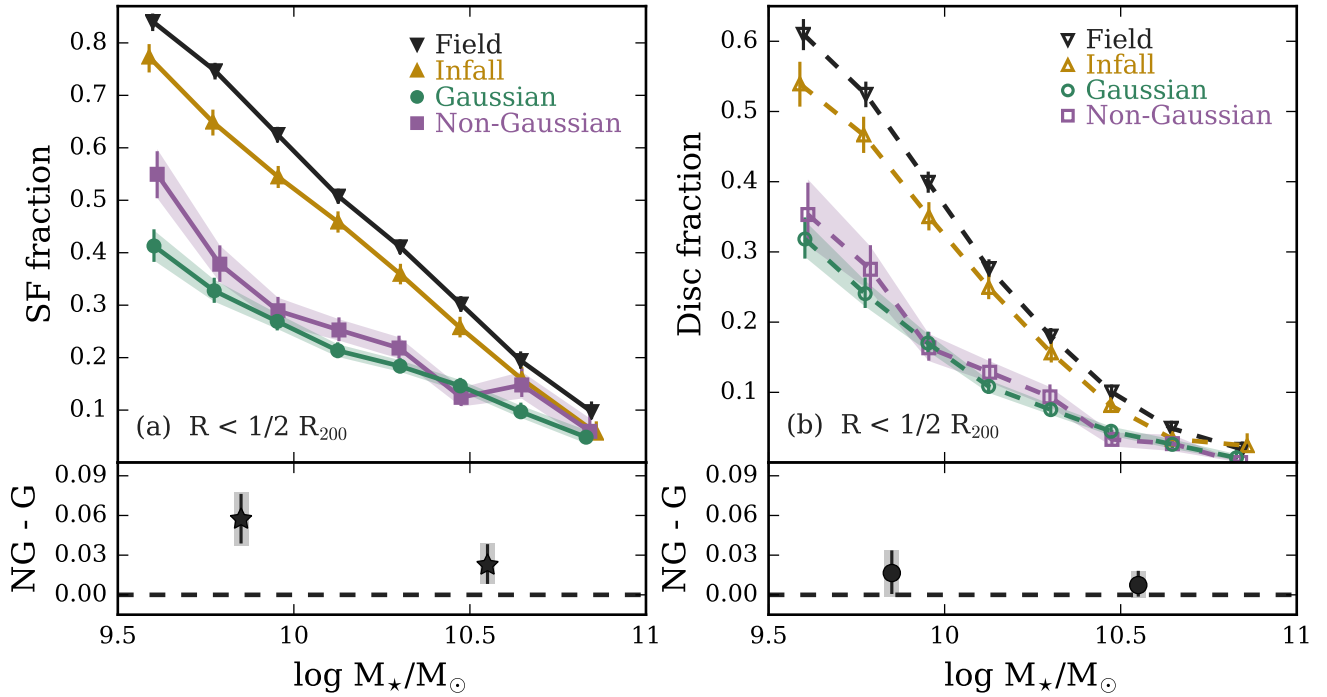


Figure 5. Star-forming (left) and disc (right) fraction versus stellar mass for field galaxies, infalling galaxies, and galaxies at small radii (within the median group-centric radius) in the G and NG samples. Error bars correspond to 68 per cent binomial confidence intervals as given in Cameron (2011), shaded regions are 68 per cent confidence intervals derived from 1000 bootstrap re-samplings over individual groups. Lower panels show the difference in star-forming/disc fractions between G and NG groups, for low-mass ($M_* \lesssim 10^{10.2} M_\odot$) and high-mass ($M_* \gtrsim 10^{10.2} M_\odot$) galaxies.

cant enhancement in NG groups for low or high mass galaxies (0.9σ and 0.8σ , respectively). As was the case for galaxies at large radii, we show results corresponding to different p-value choices in Appendix A. The observed trends do not depend strongly on p-value. If anything, choosing a larger p-value only strengthens the observed difference between G and NG at large stellar mass (see Appendix A).

5 DISCUSSION

5.1 The impact of group dynamical state

The question of how much group dynamical state influences galaxy properties has not yet been conclusively answered. In this study we find that star formation of galaxies within the inner regions of haloes show a dependence on group dynamics. In particular, we find that compared to G groups galaxies at small radii in NG groups show an increase in star-forming fraction.

Carollo et al. (2013) study the differences between galaxies in ‘relaxed’ and ‘unrelaxed’ groups (defined based upon the presence, or lack thereof, of a well defined central group galaxy) in the Zurich Environmental Study. Carollo et al. (2013) find that $< 10^{10} M_\odot$ satellites show slightly redder colours in relaxed groups compared to unrelaxed groups. Given the general correlations between galaxy colour and star formation, this agrees well with the findings of this work. Ribeiro et al. (2013a) use a statistical metric designed to

quantify the distance between probability density functions, known as the Hellinger distance, to discriminate between G and NG groups using a FOF catalogue of SDSS group galaxies (Berlind et al. 2006). They find no dependence on group dynamics for bright galaxies ($M_r \leq -20.7$), however find that properties of faint galaxies ($-20.7 < M_r \leq -17.9$) do depend on whether they live in a G or NG group. Relevant to this work, Ribeiro et al. (2013a) show that faint galaxies in G groups are redder than their NG counterparts. As well, Ribeiro et al. (2010) find that galaxies in G groups are redder than galaxies in NG groups out to $4R_{200}$.

Hou et al. (2013) have explored the dependence of quiescent fraction on group dynamical state as a function of redshift using a combination of groups from the SDSS and the Group Environment and Evolution Collaboration (GEEC). For their low redshift galaxies, Hou et al. find no difference between the quiescent fraction of galaxies in NG versus G groups, though they use a stellar mass complete sample and are only able to probe masses of $M_* > 10^{10} M_\odot$. This is consistent with the result from this work showing that any correlations with dynamical state are subtle and only seen for low-mass galaxies.

The results of this paper can be used to further constrain the connection between group dynamics and the quenching of star formation as well as morphological transformations. The main result is that we observe a dependence of star formation on dynamics in the inner region of the halo but not for galaxies at large radii, whereas mor-

phology is not found to correlate with dynamics at any radius. This seems to suggest that quenching is primarily taking place near the centres of groups, and is more efficient in G groups than NG groups. Alternatively, the observed excess of star-forming galaxies in NG groups could be due to the more dynamically complex NG groups having assembled more recently, therefore galaxies in G groups will have been exposed to quenching mechanisms within the group environment for longer.

It is also worth noting that the unusual structure in velocity space of the NG groups could be a result of poorly identified groups which have undergone ‘fusing’ (ie. two separate haloes which group finders have combined into one group) or ‘fracturing’ (ie. one distinct halo which has been split into multiple groups by group finders). Recent works (Duarte & Mamon 2014; Campbell et al. 2015) have investigated the degree to which standard group finding techniques can accurately reproduce groups from mock catalogues. Campbell et al. (2015) show that these misidentifications can bias some colour-dependent statistics, such as red fraction which is directly related to the star-forming fraction considered in this work. It would be useful in future work to apply the same statistics used here to discriminate between G and NG groups on mock catalogues in order to determine what fraction of identified NG groups are in fact unrelaxed, dynamically young systems as opposed to systems which have simply been misidentified by the group finder.

5.2 Pre-processing of infalling galaxies

In addition to star formation quenching and morphological transformations within the current host halo, we also find evidence for pre-processing in both star formation and morphology. To probe pre-processing we measure the “field excess” (ie. the degree to which star-forming and disc fractions are enhanced in the field relative to the infalling region of groups). Assuming that any environmentally driven quenching or morphological transformations occur within the virial radius of a halo, the field excess will correspond to the fraction of infalling galaxies which have been pre-processed. Using this we quantitatively determine the level of pre-processing by computing the field excess for low-mass and high-mass galaxies (divided at the median stellar mass of our sample, $M_* \gtrsim 10^{10.2} M_\odot$) in our three halo mass bins. As shown in Fig. 4, we find that the fraction of pre-processed low-mass galaxies ranges between 4 and 11 per cent when considering star-forming fraction and between 4 and 7 per cent when considering disc fraction. For high-mass galaxies the pre-processed fraction is smaller and generally only marginally significant.

Prior studies have aimed to constrain the fraction of pre-processed galaxies. One common approach is to measure the fraction of galaxies which fall onto a cluster as a member of a smaller group, either directly using simulations or by measuring substructure or clustering observationally. For clusters with mass $\sim 10^{14} M_\odot$ De Lucia et al. (2012) use semi-analytic models (SAMs) and find that the fraction of satellite galaxies which are accreted in groups with $M_H \gtrsim 10^{13} M_\odot$ is highest for low-mass galaxies, corresponding to ~ 28 per cent. Also using SAMs, McGee et al. (2009) find that the fraction of galaxies accreted onto the ultimate cluster as members of $\gtrsim 10^{13} h^{-1} M_\odot$ groups de-

pends strongly on the cluster halo mass, ranging from ~ 0.1 for $10^{13.5} h^{-1} M_\odot$ haloes to ~ 0.45 for haloes with masses of $10^{15} h^{-1} M_\odot$. Bahé et al. (2013) use the GIMIC suite of zoom-in simulations and find that the fraction of galaxies which have been satellites of a $> 10^{13} M_\odot$ halo prior to accretion onto the ultimate host ranges from < 10 per cent for a host with halo mass $< 10^{13.5} M_\odot$, up to as high as ~ 60 per cent for a host halo mass of $10^{15.2} M_\odot$. Observationally, Hou et al. (2014) use the Dressler-Schechter test (Dressler & Schechter 1988) to identify infalling subhaloes and find for $< 10^{14} M_\odot$ groups that less than 5 per cent of infalling galaxies are part of a subhalo, whereas for haloes with masses $10^{14} < M_H < 10^{14.5} M_\odot$ and $M_H > 10^{14.5} M_\odot$ the fraction of galaxies infalling in subhaloes is ~ 10 per cent and ~ 25 per cent, respectively. Qualitatively the pre-processing trends observed in this work are consistent with these previous studies, namely the fraction of pre-processed galaxies tends to decrease with increasing galaxy stellar mass and increase with the halo mass of the host which the galaxies are infalling onto. The subhalo fraction found in these works can be interpreted as an upper limit on the field excess quantity which we quote. This is because only some fraction of galaxies within subhaloes during infall will be pre-processed, whereas the field excess more closely measures the fraction of galaxies which have actually been pre-processed. Therefore the fact that our values for the fraction of pre-processed galaxies are consistently smaller than the quoted subhalo fractions is still consistent.

Studying the star-forming fractions of cluster galaxies, Haines et al. (2015) use a simple toy model in an attempt to reproduce the trend between cluster-centric radius and star-forming fraction. They find that in order to reproduce the observational trend, a 19 per cent decrease in the star-forming fraction of cluster galaxies relative to the field is required on top of star formation quenching occurring within the virial radius. Haines et al. suggest that pre-processing is a possible mechanism to generate this 19 per cent decrease. In this work we find that the fraction of high-mass (the Haines et al. sample consists of galaxy stellar masses $> 2 \times 10^{10.2} M_\odot$) pre-processed galaxies for high-mass clusters is at most 7 ± 2 per cent. Therefore, this work is only able to account for a portion of the amount of pre-processing required by the Haines et al. (2015) model, although a more complete comparison would require samples matched in halo mass and galaxy stellar mass.

At $\sim z = 0.2$, Lu et al. (2012) find that blue fractions of low and intermediate-mass cluster galaxies are lower than the field values (at the same stellar mass) out to radii of 7 Mpc, however the most massive galaxies show no difference from the field. This is similar to the stellar mass trends observed in this work where we see stronger pre-processing for low-mass galaxies.

Recent studies have examined pre-processing of morphology (e.g. Kodama & Smail 2001; Helsdon & Ponman 2003; Moran et al. 2007; Wilman et al. 2009) and star formation (e.g. Cortese et al. 2006; Wetzel et al. 2012; Bahé et al. 2013; Haines et al. 2015) separately, however we are not aware of other works which have made direct quantitative comparisons between the amount of pre-processing of star formation versus morphology. In Fig. 4 we see evidence for pre-processing in both star formation and morphology, though due to the relatively large errorbars it is unclear

whether one is more strongly pre-processed than the other. The largest difference between star formation and morphology is in the highest halo mass bin, where star formation shows marginally stronger pre-processing than morphology. Additionally if we consider the entire data set (without subdividing by halo mass) we find that the pre-processing of star formation rate is marginally enhanced relative to morphology at the $\sim 2\sigma$ level. Understanding the relative strength of pre-processing of star formation versus morphology could help to disentangle environmentally driven galaxy evolution mechanisms and should be explored further.

6 SUMMARY & CONCLUSIONS

In this paper we investigate the dependence of galaxy properties (namely, star-forming and disc fractions) on host group dynamics. To do so we construct a carefully matched sample of galaxies housed in Gaussian groups, galaxies housed in non-Gaussian groups, as well as infalling and field galaxies; all with similar distributions in stellar mass, redshift, and (field galaxies excluded) halo mass. We then compare the properties of these different samples for two different radial regions within the halo. The main findings of this work are as follows:

1. Star-forming and disc fractions of galaxies at large group-centric radius do not show any dependence on the dynamical state of their host group
2. We detect pre-processing by measuring the difference between the star-forming and disc fractions for field galaxies compared to infalling galaxies. Infalling galaxies have had both star formation and morphology pre-processed, with low-mass galaxies infalling onto high-mass haloes showing the largest degree of pre-processing.
3. Galaxy star-formation in the inner region of the halo shows a clear dependence on group dynamical state, with enhanced star-forming fractions for galaxies in non-Gaussian groups compared to galaxies in Gaussian groups at the same stellar mass. We do not detect a significant dependence of disc fraction on group dynamical state in the same inner region.

ACKNOWLEDGMENTS

We thank the referee for their insightful comments and suggestions, which have improved this paper significantly. IDR thanks the Ontario Graduate Scholarship program and the National Science and Engineering Research Council of Canada for funding. LCP thanks the National Science and Engineering Research Council of Canada for funding. The authors thank F. Evans for matching together the various SDSS catalogues used in this research. We thank X. Yang et al. for making their SDSS DR7 group catalogue publicly available, L. Simard et al. for the publication of their SDSS DR7 morphology catalogue, J. Brinchmann et al. for publication of their SDSS SFRs, and the NYU-VAGC team for the publication of their SDSS DR7 catalogue. This research would not have been possible without access to these public catalogues.

Funding for the SDSS has been provided by the Alfred P. Sloan Foundation, the Participating Institutions, the

National Science Foundation, the U.S. Department of Energy, the National Aeronautics and Space Administration, the Japanese Monbukagakusho, the Max Planck Society, and the Higher Education Funding Council for England. The SDSS Web Site is <http://www.sdss.org/>.

The SDSS is managed by the Astrophysical Research Consortium for the Participating Institutions. The Participating Institutions are the American Museum of Natural History, Astrophysical Institute Potsdam, University of Basel, University of Cambridge, Case Western Reserve University, University of Chicago, Drexel University, Fermilab, the Institute for Advanced Study, the Japan Participation Group, Johns Hopkins University, the Joint Institute for Nuclear Astrophysics, the Kavli Institute for Particle Astrophysics and Cosmology, the Korean Scientist Group, the Chinese Academy of Sciences (LAMOST), Los Alamos National Laboratory, the Max-Planck-Institute for Astronomy (MPIA), the Max-Planck-Institute for Astrophysics (MPA), New Mexico State University, Ohio State University, University of Pittsburgh, University of Portsmouth, Princeton University, the United States Naval Observatory, and the University of Washington.

REFERENCES

- Abazajian K. N., et al., 2009, *ApJS*, 182, 543
 Anderson T. W., Darling D. A., 1952, *The Annals of Mathematical Statistics*, 23, 193
 Ashman K. M., Bird C. M., Zepf S. E., 1994, *AJ*, 108, 2348
 Bahé Y. M., McCarthy I. G., Balogh M. L., Font A. S., 2013, *MNRAS*, 430, 3017
 Bamford S. P., et al., 2009, *MNRAS*, 393, 1324
 Berlind A. A., et al., 2006, *ApJS*, 167, 1
 Bird C. M., Beers T. C., 1993, *AJ*, 105, 1596
 Biviano A., Katgert P., Thomas T., Adami C., 2002, *A&A*, 387, 8
 Blanton M. R., Roweis S., 2007, *AJ*, 133, 734
 Blanton M. R., et al., 2005, *AJ*, 129, 2562
 Brinchmann J., Charlot S., White S. D. M., Tremonti C., Kauffmann G., Heckman T., Brinkmann J., 2004, *MNRAS*, 351, 1151
 Butcher H., Oemler Jr. A., 1978, *ApJ*, 226, 559
 Cameron E., 2011, *PASA*, 28, 128
 Campbell D., van den Bosch F. C., Hearin A., Padmanabhan N., Berlind A., Mo H. J., Tinker J., Yang X., 2015, *MNRAS*, 452, 444
 Carollo C. M., et al., 2013, *ApJ*, 776, 71
 Christlein D., Zabludoff A. I., 2004, *ApJ*, 616, 192
 Cortese L., Gavazzi G., Boselli A., Franzetti P., Kennicutt R. C., O’Neil K., Sakai S., 2006, *A&A*, 453, 847
 Cucciati O., et al., 2012, *A&A*, 539, A31
 De Lucia G., Fontanot F., Wilman D., 2012, *MNRAS*, 419, 1324
 Dressler A., 1980, *ApJ*, 236, 351
 Dressler A., Shectman S. A., 1988, *AJ*, 95, 985
 Dressler A., Smail I., Poggianti B. M., Butcher H., Couch W. J., Ellis R. S., Oemler Jr. A., 1999, *ApJS*, 122, 51
 Dressler A., Oemler Jr. A., Poggianti B. M., Gladders M. D., Abramson L., Vulcani B., 2013, *ApJ*, 770, 62
 Duarte M., Mamon G. A., 2014, *MNRAS*, 440, 1763
 Eke V. R., Baugh C. M., Cole S., Frenk C. S., King H. M., Peacock J. A., 2005, *MNRAS*, 362, 1233
 Fasano G., et al., 2015, *MNRAS*, 449, 3927
 Feulner G., Gabasch A., Salvato M., Drory N., Hopp U., Bender R., 2005, *ApJ*, 633, L9

Fillingham S. P., Cooper M. C., Wheeler C., Garrison-Kimmel S., Boylan-Kolchin M., Bullock J. S., 2015, *MNRAS*, 454, 2039

Fujita Y., 2004, *PASJ*, 56, 29

Geller M. J., Huchra J. P., 1983, *ApJS*, 52, 61

Goto T., Yamauchi C., Fujita Y., Okamura S., Sekiguchi M., Smail I., Bernardi M., Gomez P. L., 2003, *MNRAS*, 346, 601

Gray M. E., Wolf C., Meisenheimer K., Taylor A., Dye S., Borch A., Kleinheinrich M., 2004, *MNRAS*, 347, L73

Gunn J. E., Gott III J. R., 1972, *ApJ*, 176, 1

Haines C. P., La Barbera F., Mercurio A., Merluzzi P., Busarello G., 2006, *ApJ*, 647, L21

Haines C. P., et al., 2015, *ApJ*, 806, 101

Hartigan J. A., Hartigan P. M., 1985, *The Annals of Statistics*, 13, 70

Helsdon S. F., Ponman T. J., 2003, *MNRAS*, 339, L29

Hou A., Parker L. C., Harris W. E., Wilman D. J., 2009, *ApJ*, 702, 1199

Hou A., et al., 2013, *MNRAS*, 435, 1715

Hou A., Parker L. C., Harris W. E., 2014, *MNRAS*, 442, 406

Hubble E., Humason M. L., 1931, *ApJ*, 74, 43

Huchra J. P., Geller M. J., 1982, *ApJ*, 257, 423

Just D. W., et al., 2015, preprint, ([arXiv:1506.02051](https://arxiv.org/abs/1506.02051))

Kawata D., Mulchaey J. S., 2008, *ApJL*, 672, L103

Kodama T., Smail I., 2001, *MNRAS*, 326, 637

Lackner C. N., Gunn J. E., 2013, *MNRAS*, 428, 2141

Lewis I., et al., 2002, *MNRAS*, 334, 673

Lu T., Gilbank D. G., McGee S. L., Balogh M. L., Gallagher S., 2012, *MNRAS*, 420, 126

Mahajan S., Mamon G. A., Raychaudhury S., 2011, *MNRAS*, 416, 2882

Mamon G. A., Sanchis T., Salvador-Solé E., Solanes J. M., 2004, *A&A*, 414, 445

Martínez H. J., Zandivarez A., 2012, *MNRAS*, 419, L24

McGee S. L., Balogh M. L., Bower R. G., Font A. S., McCarthy I. G., 2009, *MNRAS*, 400, 937

McGee S. L., Balogh M. L., Wilman D. J., Bower R. G., Mulchaey J. S., Parker L. C., Oemler A., 2011, *MNRAS*, 413, 996

Mihos J. C., Hernquist L., 1994, *ApJ*, 425, L13

Mo H. J., White S. D. M., 1996, *MNRAS*, 282, 347

Moore B., Katz N., Lake G., Dressler A., Oemler A., 1996, *Nature*, 379, 613

Moran S. M., Ellis R. S., Treu T., Smith G. P., Rich R. M., Smail I., 2007, *ApJ*, 671, 1503

Muzzin A., et al., 2014, *ApJ*, 796, 65

Navarro J. F., Frenk C. S., White S. D. M., 1997, *ApJ*, 490, 493

Oman K. A., Hudson M. J., Behroozi P. S., 2013, *MNRAS*, 431, 2307

Peng Y.-j., et al., 2010, *ApJ*, 721, 193

Peng Y., Maiolino R., Cochrane R., 2015, *Nature*, 521, 192

Popesso P., Biviano A., Böhringer H., Romaniello M., 2007, *A&A*, 461, 397

Postman M., Geller M. J., 1984, *ApJ*, 281, 95

Postman M., et al., 2005, *ApJ*, 623, 721

Rasmussen J., Mulchaey J. S., Bai L., Ponman T. J., Raychaudhury S., Dariush A., 2012, *ApJ*, 757, 122

Razali N. M., Wah Y. B., 2011, *Journal of Statistical Modeling and Analytics*, 2, 21

Ribeiro A. L. B., Lopes P. A. A., Trevisan M., 2010, *MNRAS*, 409, L124

Ribeiro A. L. B., de Carvalho R. R., Trevisan M., Capelato H. V., La Barbera F., Lopes P. A. A., Schilling A. C., 2013a, *MNRAS*, 434, 784

Ribeiro A. L. B., Lopes P. A. A., Rembold S. B., 2013b, *A&A*, 556, A74

Rines K., Geller M. J., Kurtz M. J., Diaferio A., 2005, *AJ*, 130, 1482

Roberts I. D., Parker L. C., Karunakaran A., 2016, *MNRAS*, 455, 3628

Schawinski K., Virani S., Simmons B., Urry C. M., Treister E., Kaviraj S., Kushkuley B., 2009, *ApJL*, 692, L19

Simard L., Mendel J. T., Patton D. R., Ellison S. L., McConnachie A. W., 2011, *ApJS*, 196, 11

Skibba R. A., van den Bosch F. C., Yang X., More S., Mo H., Fontanot F., 2011, *MNRAS*, 410, 417

Tasca L. A. M., et al., 2014, *A&A*, 564, L12

Taylor E. N., et al., 2011, *MNRAS*, 418, 1587

Tinker J., Kravtsov A. V., Klypin A., Abazajian K., Warren M., Yepes G., Gottlöber S., Holz D. E., 2008, *ApJ*, 688, 709

Verdugo M., Ziegler B. L., Gerken B., 2008, *A&A*, 486, 9

Wang Y., Yang X., Mo H. J., van den Bosch F. C., Weinmann S. M., Chu Y., 2008, *ApJ*, 687, 919

Weisz D. R., Dolphin A. E., Skillman E. D., Holtzman J., Gilbert K. M., Dalcanton J. J., Williams B. F., 2015, *ApJ*, 804, 136

Wetzel A. R., Tinker J. L., Conroy C., 2012, *MNRAS*, 424, 232

Wetzel A. R., Tollerud E. J., Weisz D. R., 2015, *ApJ*, 808, L27

Whitmore B. C., Gilmore D. M., Jones C., 1993, *ApJ*, 407, 489

Wilman D. J., et al., 2005, *MNRAS*, 358, 88

Wilman D. J., Oemler Jr. A., Mulchaey J. S., McGee S. L., Balogh M. L., Bower R. G., 2009, *ApJ*, 692, 298

Yahil A., Vidal N. V., 1977, *ApJ*, 214, 347

Yang X., Mo H. J., van den Bosch F. C., Jing Y. P., 2005, *MNRAS*, 356, 1293

Yang X., Mo H. J., van den Bosch F. C., Pasquali A., Li C., Barden M., 2007, *ApJ*, 671, 153

Zheng X. Z., Bell E. F., Papovich C., Wolf C., Meisenheimer K., Rix H.-W., Rieke G. H., Somerville R., 2007, *ApJ*, 661, L41

APPENDIX A: DEPENDENCE ON THE DEFINITION OF NG GROUPS

To discriminate between G and NG groups we use a critical p-value of 0.05 for both the AD test and the Dip test (see Section 2.3). While this choice of 0.05 is standard, it is still an arbitrary choice and it is therefore important to investigate the effect of varying this dividing p-value.

Figs A1 and A2 show star-forming and disc fractions for galaxies in the outer and inner regions of G and NG groups (similar to Figs 3 and 5), for different choices of the dividing p-value between G and NG groups. The lower panels in Figs 3 and 5 show NG – G for different choices of p-value, with the height of the data marker corresponding to 68 per cent confidence intervals derived from either bootstrapping or the methodology of Cameron (2011) (whichever is larger). Please note that the data markers are offset from one another for visibility. Lines range in decreasing transparency from p-values of 0.05 to 0.20.

We see no indication that the results of this work are strongly sensitive to the choice of p-value, as qualitatively similar trends are observed for all p-values shown in Figs A1 and A2. Quantitatively, no enhancement of disc fractions in NG groups is seen above the 2σ level at large or small radius (and for large or small stellar mass), with the exception of the $p < 0.10$ sample at small stellar mass where an enhancement of 2.1σ is detected. Considering star-forming fractions at small radius we see a similar enhancement of star-forming fractions in NG groups for low-mass galaxies, significant at $> 2\sigma$ for all p-values. For high-mass galaxies, an enhancement at the 2σ level is detected for the $p < 0.10$, $p < 0.15$, and $p < 0.20$ cases whereas the 2σ level was not reached for the $p < 0.05$ sample used in the paper. This is primarily due to uncertainties on the fractions in the NG sample becom-

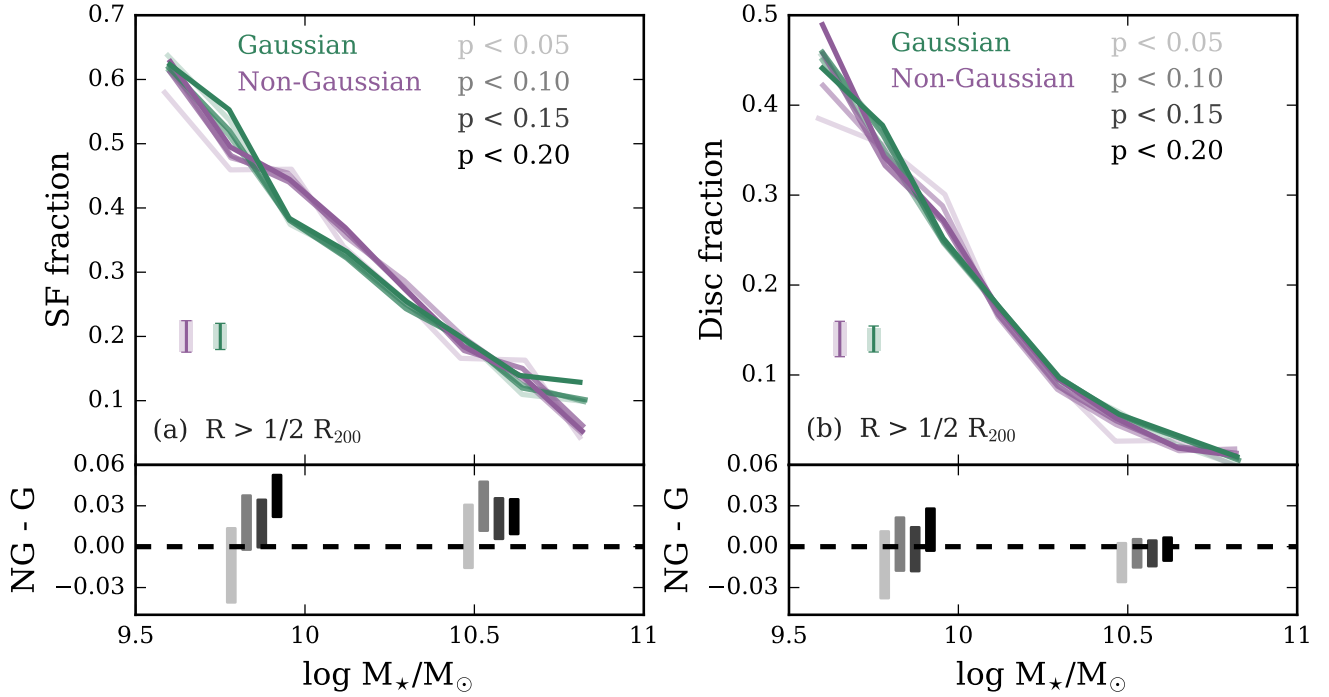


Figure A1. Star-forming (left) and disc (right) fraction versus stellar mass for galaxies at large radius in the G and NG samples. The lines of varying transparency correspond to different definitions of the NG sample, where the listed p-value is the critical value used in the AD and Dip tests to identify NG groups. Characteristic uncertainties are shown for 68 per cent confidence intervals from Cameron (2011) (errorbars) and from 1000 bootstrap re-samplings (shaded regions). Lower panels show the difference between star-forming fractions in G and NG groups (left) and similarly for disc fraction (right), for low-mass ($M_{\star} \lesssim 10^{10.2} M_{\odot}$) and high-mass ($M_{\star} \gtrsim 10^{10.2} M_{\odot}$) galaxies.

ing smaller as the dividing p-value is increased (leading to a larger NG sample). For star-forming fractions at large radius an enhancement in NG groups is only detected at $> 2\sigma$ in the $p < 0.20$ case for low-mass galaxies, and no enhancement is detected in any case for high-mass galaxies. These trends with star-forming and disc fractions are generally consistent with the trends presented in the body of the paper, with any differences only strengthening the conclusion that star formation is enhanced in NG groups relative to G groups.

This paper has been typeset from a \LaTeX file prepared by the author.

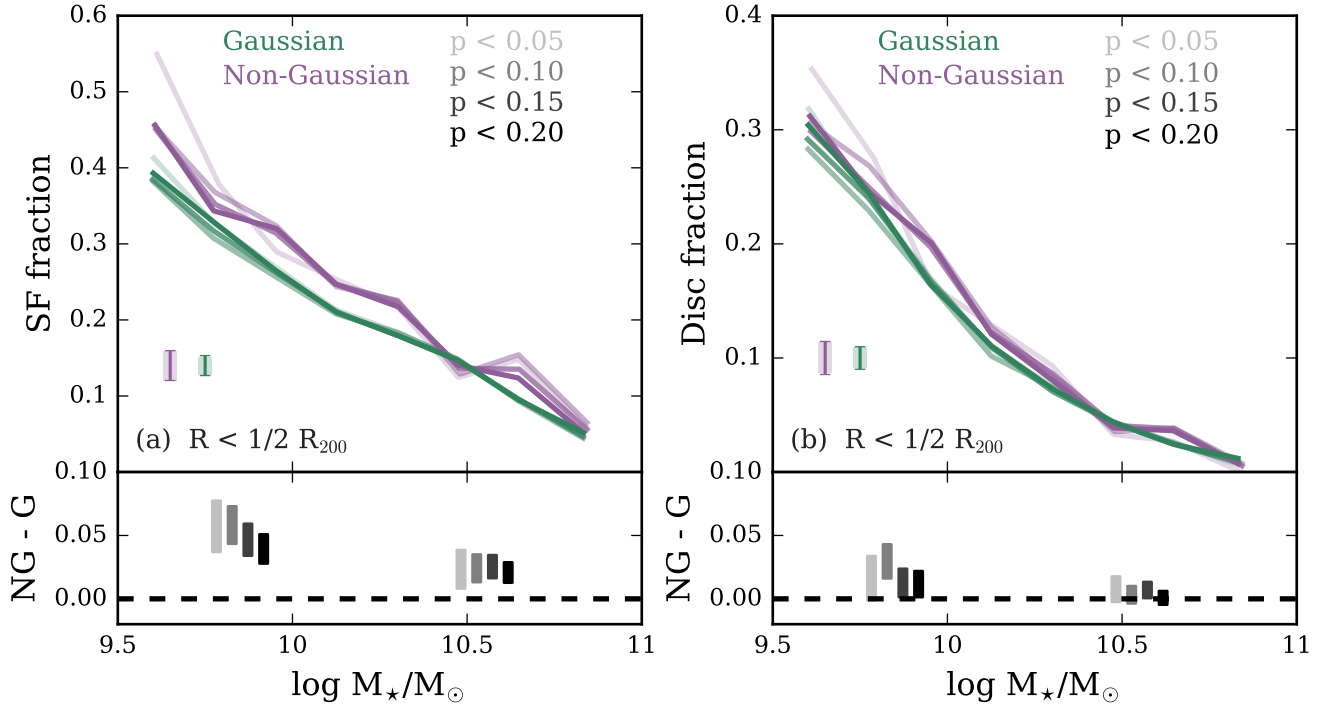


Figure A2. Star-forming (left) and disc (right) fraction versus stellar mass for galaxies at small radius in the G and NG samples. The lines of varying transparency correspond to different definitions of the NG sample, where the listed p-value is the critical value used in the AD and Dip tests to identify NG groups. Characteristic uncertainties are shown for 68 per cent confidence intervals from Cameron (2011) (errorbars) and from 1000 bootstrap re-samplings (shaded regions). Lower panels show the difference between star-forming fractions in G and NG groups (left) and similarly for disc fraction (right), for low-mass ($M_* \lesssim 10^{10.2} M_\odot$) and high-mass ($M_* \gtrsim 10^{10.2} M_\odot$) galaxies.